

Self-consistent electronic structures of magnetic semiconductors by a discrete variational $X\alpha$ calculation. III. Chalcopyrite CuFeS_2

Toshiki Hamajima, Takeshi Kambara,* and Ken Ichiro Gondaira

Department of Engineering Physics, The University of Electro-Communications, Chofu, Tokyo 182, Japan

Tamio Oguchi

Institute for Solid State Physics, The University of Tokyo, Minatoku, Tokyo 106, Japan

(Received 20 March 1981)

The electronic band structure of chalcopyrite CuFeS_2 in the antiferromagnetic phase is calculated by spin-polarized self-consistent-charge discrete-variational $X\alpha$ method. The valence bands consist of many rather narrow bands constructed from S $3p$, Cu $3d$, and majority-spin Fe $3d$ orbitals. The upper valence bands are constituted mainly of Cu $3d$ and Fe $3d$ orbitals. The top of the valence band is at the X point. The conduction bands composed mainly of $4s$ and $4p$ orbitals of Cu and Fe have the bottom at the Γ point and the direct gap is 3.1 eV. The narrow bands composed mainly of minority-spin Fe $3d$ orbitals are in the so-called fundamental gap. The direct minimum gap of these d bands is 0.7 eV at the X point. These gap energies are in good agreement with the observed optical spectra. The minimum gap of the minority-spin d bands is indirect and about 0.3 eV. The magnetic moment of an Fe ion is $3.88\mu_B$, which agrees with the observed value.

I. INTRODUCTION

Chalcopyrite CuFeS_2 is the unique magnetic semiconductor among the ternary semiconductors with chalcopyrite structure. The optical and electrical properties of CuFeS_2 are quite different from those of other chalcopyrite-type semiconductors: The energy of the optical absorption edge is very small compared with that of the other compounds,¹⁻³ the temperature dependence of electric conductivity shows a metallic behavior,⁴ but the electron mobility is very low for both n - and p -type samples.^{4,5} Furthermore, CuFeS_2 shows several interesting magnetic properties which are quite different from the properties of usual insulating magnets: The effective magnetic moment $3.85\mu_B$ of the Fe ion⁶ is neither the value of Fe^{3+} nor that of Fe^{2+} and the Néel temperature is very high; the magnetic susceptibility has no temperature dependence.^{5,7}

It has been made clear through the persistent investigation of Teranishi and Sato that those characteristic features of CuFeS_2 arise mainly from the delocalization of the $3d$ electrons of Fe: The d bands with minority spin are in the so-called fundamental gap between the valence band and the conduction band constructed with $4s$ and $4p$ orbitals of Cu and Fe. The $3d$ orbitals of Cu and Fe ions mix

considerably into the upper valence bands. That is, carriers in both n - and p -types samples have a strong d -electron character. The metallic behavior in the electric conduction has been explained by assuming that CuFeS_2 is a degenerate semiconductor.⁴ However, the measurement of the Mössbauer effect showed that an Fe ion in CuFeS_2 is in the trivalent state.⁸ This could not be explained from the delocalization model.

Previously, we calculated the electronic structure of CuFeS_2 clusters by the molecular-orbital method⁹ and also by the valence-bond method¹⁰ to take into account the many-body effects, in order to clarify such complicated states of $3d$ electrons of Fe. In the present paper, we calculate self-consistently the electronic band structure of antiferromagnetic CuFeS_2 by using the spin-polarized self-consistent-charge discrete-variational (DV)- $X\alpha$ method¹¹⁻¹³ in order to obtain further quantitative information about the delocalization of iron d electrons.

II. CALCULATION METHOD

Since the DV- $X\alpha$ method we used was described in detail in the previous paper,¹⁴ we give here only the data relevant to this calculation. The crystal

structure of chalcopyrite CuFeS_2 is shown in Fig. 1. The unit cell contains two molecules (2 CuFeS_2). The space group of this crystal is $D_{2d}^{12}(\bar{I}43m)$ in the paramagnetic phase and $S_4^2(\bar{I}4)$ in the antiferromagnetic phase as shown in Fig. 1. We use the numerically generated atomic orbitals as the basis function, specifically, $1s-4p$ for Cu and Fe, and $1s-3p$ for S. The exchange scaling parameter α of the $X\alpha$ potential is fixed to 0.7 and we use a total of 2000 sample points in the unit cell for integration to get the matrix elements. The self-consistent-charge iterative procedure¹⁵ is employed and as the criterion for the self-consistency we require that the discrepancy between the input and output populations of atomic orbitals be less than 0.02. The accuracy of the calculated energy values is ± 0.2 eV.

III. RESULTS

The calculated bands $\Gamma\Delta X$ and $\Gamma\Lambda Z$ corresponding to the Brillouin zone in Fig. 2 are shown in Fig.

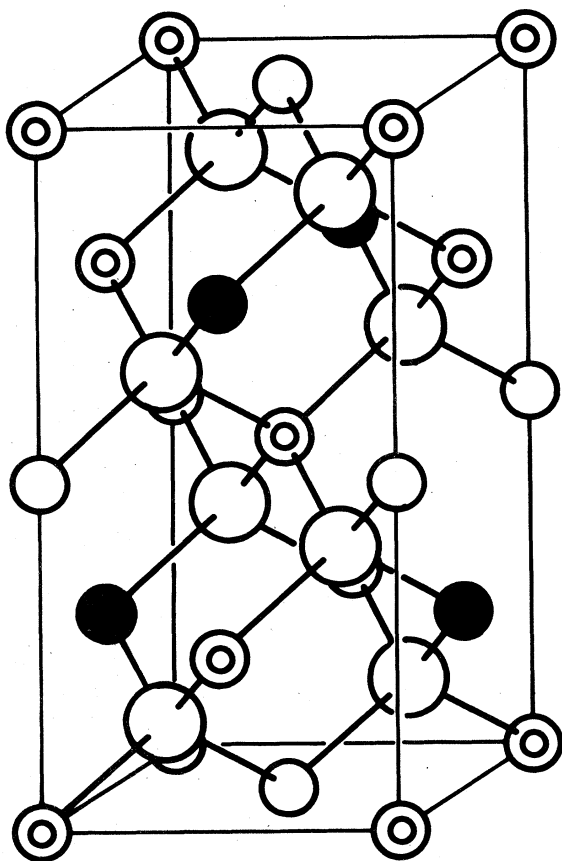


FIG. 1. Crystal structure of CuFeS_2 . The large white circle denotes S, the double Cu, the small white Fe_I , and the black Fe_{II} . The Bravais lattice is body-center tetragonal.

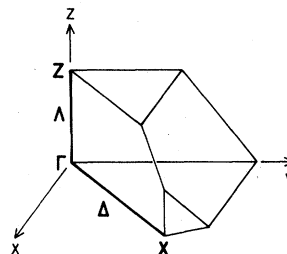


FIG. 2. The $\frac{1}{16}$ irreducible part of the Brillouin zone for the chalcopyrite structure.

3. The Fermi level is taken as the zero of the energy scale. There are many bands connected with a large number of constituent atoms in the unit cell, and, consequently, a large number of basis functions: The unit cell contains two formula units, that is, eight atoms. The bands around and below the Fermi level include d -orbital components of Fe and Cu and have a small dispersion.

The energy eigenvalues and the detailed atomic contents of the wave functions of all the bands shown in Fig. 3 are listed in Table I for the Γ point.¹⁶ There are two inequivalent Fe atoms in the unit cell which have opposite spin directions in the antiferromagnetic phase. Denote as Fe_I the atom whose up-spin states are almost filled and the other

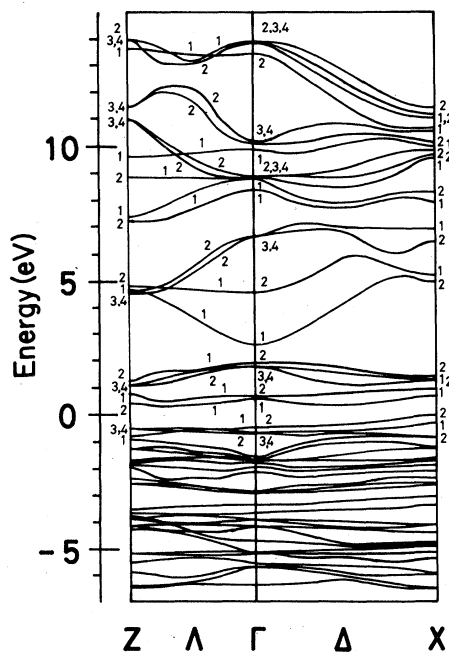


FIG. 3. Calculated band structure with a given spin-direction of antiferromagnetic CuFeS_2 . The figures attached to the bands denote the symmetry of the levels.

TABLE I. The eigenvalues and atomic contents of the up-spin eigenfunctions at the Γ point. The blank means less than 5%. The Fermi level is 0.00 eV. The notation of the group representations follows Ref. 19.

Symmetry	Energy (eV)	Cu		Fe _I		Fe _{II}		S	
3,4	13.86	<i>p</i>	34	<i>p</i>	19	<i>p</i>	30	<i>p</i>	16
2	13.83	<i>p</i>	35			<i>p</i>	45	<i>p</i>	18
2	13.38	<i>p</i>	41	<i>p</i>	36			<i>p</i>	21
3,4	10.08	<i>p</i>	48	<i>p</i>	14	<i>p</i>	32		
1	9.84					<i>s</i>	63	<i>p</i>	26
2	8.88	<i>p</i>	54	<i>p</i>	22	<i>p</i>	23		
3,4	8.85	<i>p</i>	47	<i>p</i>	33	<i>p</i>	18		
1	8.79	<i>s</i>	24	<i>s</i>	43			<i>p</i>	33
1	8.39	<i>s</i>	64					<i>p</i>	29
3,4	6.67	<i>p</i>	43	<i>p</i>	16			<i>p</i>	26
2	4.54	<i>p</i>	42	<i>p</i>	23	<i>p</i>	13		
1	2.65	<i>s</i>	50	<i>s</i>	18	<i>s</i>	13	<i>p</i>	19
2	1.91	<i>d</i>	10			<i>d</i> ϵ	44	<i>p</i>	37
3,4	1.80	<i>d</i>	12			<i>d</i> ϵ	45	<i>p</i>	37
2	0.71					<i>d</i> γ	89		
1	0.61					<i>d</i> γ	96		
2	-0.45	<i>d</i> ϵ	42			<i>d</i> ϵ	29	<i>p</i>	18
3,4	-0.65	<i>d</i> ϵ	35			<i>d</i> ϵ	36	<i>p</i>	17
2	-1.53	<i>d</i> γ	81						
2	-1.62	<i>d</i> γ	76			<i>d</i>	10		
3,4	-1.66	<i>d</i> ϵ	76					<i>p</i>	10
1	-1.76	<i>d</i> γ	92						
1	-1.94	<i>d</i> γ	97						
2	-2.13	<i>d</i> ϵ	94						
2	-2.82	<i>d</i> ϵ	38	<i>d</i> ϵ	37			<i>p</i>	14
3,4	-2.86	<i>d</i>	39	<i>d</i>	30			<i>p</i>	14
2	-3.35	<i>d</i>	17	<i>d</i> γ	67			<i>p</i>	13
1	-3.66			<i>d</i> γ	81			<i>p</i>	10
3,4	-3.91	<i>p</i>	10					<i>p</i>	73
3,4	-4.15	<i>d</i>	17					<i>p</i>	67
2	-4.68	<i>d</i>	20	<i>d</i> ϵ	25			<i>p</i>	46
1	-5.12	<i>s</i>	15			<i>s</i>	12	<i>p</i>	70
3,4	-5.15			<i>d</i> ϵ	52			<i>p</i>	37
2	-5.54			<i>d</i>	25			<i>p</i>	57
1	-5.64	<i>s</i>	12					<i>p</i>	63
2	-5.66			<i>d</i>	30			<i>p</i>	54
1	-6.33			<i>d</i>	10			<i>p</i>	65

atom as Fe_{II}. We present the result only for up-spin states in this table and thereafter. As for down-spin orbitals, the roles of Fe_I and Fe_{II} interchange.

The valence bands are composed mainly of the 3*p* orbitals of S and the 3*d* of both Cu and Fe_I. The levels, of which the 3*p* orbitals of S are the major portion, are relatively deep; they range from -6.5 to -3.8 eV for all of the Γ , *X*, and *Z* points. A few levels have the 3*d* orbitals of Fe_I as the main component; they are at -5.2, -3.7, and -3.4 eV for the Γ point and not very different for other *k*

points. Most upper valence bands contain the Cu 3*d* orbitals as the major component. A few levels immediately below the Fermi level contain the Fe_{II} 3*d* as a relatively large component. Levels constructed from almost pure Fe_{II} 3*d* (*d* γ) and levels including Fe_{II} 3*d* (*d* ϵ) as the major part, range over about 1.9 eV immediately above the Fermi level. It is the most prominent feature of this substance that the Fe_{II} 3*d* bands lie in the low-energy region with a small gap above the filled bands. True conduction bands composed mainly of 4*s* and 4*p* orbitals of Cu and Fe (both Fe_I and Fe_{II}) have the bottom at 2.65

TABLE II. The direct gap energy for each \vec{k} point. Minimum indirect gap = 0.30 eV ($X-\Lambda_3$).

k point:	Z	—	Λ	—	Γ	—	Δ	—	X
$E_F-d\gamma$	0.93	0.81	0.92	1.01	1.06	0.86	0.75	0.71	0.72
	1.28	1.01	1.14	1.24	1.16	1.18	1.17	1.07	0.97
$E_F-d\epsilon+p$	1.62	1.66	1.97	2.24	2.25	1.85	1.47	1.37	1.33
		1.84	2.13	2.38		2.18	1.90	1.56	1.35
	1.80	2.11	2.20		2.36	2.35	2.04	1.67	1.48
Fundamental gap	5.06	4.83	4.21	3.56	3.10	3.62	4.51	5.33	4.96

eV at the Γ point and a width greater than 10 eV.

The characteristic data of the band structure are tabulated in Table II. The top of the valence band has the X_2 symmetry and just touches the Fermi level. The conduction-band bottom at Γ_1 defines the fundamental indirect gap 2.65 eV while the direct energy gap at the Γ point is about 3.1 eV. As mentioned above, bands composed mainly of the minority spin $3d$ orbitals of Fe lie in the fundamental gap. The minimum of these d bands is the Λ_1 state at a point three-fourths of the way from Γ to Z, and so the smallest gap at these d bands from the top of the valence band is indirect and about 0.30 eV.

We list the self-consistent-charge population of the outer orbitals of each atom in Table III. The nominal valency of each ion is quite small. Since some ambiguity is inevitable about to which atom the charge in the intermediate regions belongs, however, the small nominal valency does not necessarily mean that this substance is very covalent and all atoms in the crystal are nearly neutral. The spin polarization of each atom can also be seen from Table III. The net magnetic moment of the

TABLE III. Self-consistent Mulliken charge populations of each atomic shell.

		Majority spin	Minority spin
Cu	$3d$	4.82	4.81
	$4s$	0.27	0.27
	$4p$	0.38	0.38
Fe	$3d$	4.88	1.24
	$4s$	0.30	0.24
	$4p$	0.47	0.29
S	$3s$	0.91	0.91
	$3p$	2.26	2.24

Fe ion is $3.88\mu_B$ and those of Cu and S are zero within the accuracy of the present calculation.

Finally, the wave-vector dependence of charge populations is shown in Fig. 4. The dependence is seen to be very small except for that of the minority spin $3d$ orbitals of Fe: Those orbitals are considerably mixed into the levels quite close to the Fermi level. The fraction of these orbitals in the highest occupied level varies strongly with \vec{k} , and the \vec{k} dependence is directly reflected in their orbital populations.

IV. DISCUSSION

In this section we compare the calculated results with the observed data and discuss the origin of the characteristic features of the electric and magnetic properties of CuFeS_2 on the basis of the calculated electronic structure.

The calculated optical transition energies at the high-symmetry points in the Brillouin zone are list-

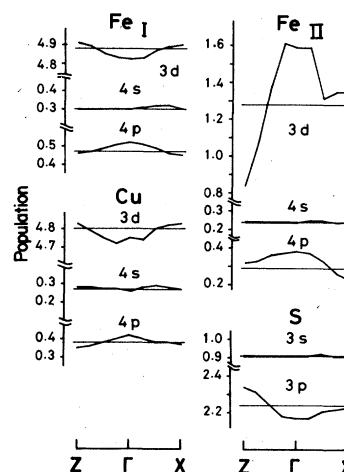


FIG. 4. \vec{k} dependence of the Mulliken charge population. Horizontal lines indicate the values averaged over \vec{k} .

ed in Table II. The energy of absorption edge is 0.72 eV at the X point and is close to the observed one of 0.6 eV.^{17,18} The energy of the fundamental absorption edge is 3.10 eV at the Γ point and is in good agreement with the observed one of 3.2 eV.¹⁸ The broad absorption bands observed below the fundamental absorption edge are assigned quite reasonably to the transitions from the uppermost valence band to the minority-spin d bands. The calculated band structure agrees quite well with the schematic energy diagram estimated from the optical spectra by Oguchi, Sato, and Teranishi.¹⁸ The calculated magnetic moment of an Fe ion is $3.88\mu_B$, remarkably close to the observed value of $3.85\mu_B$.⁶ The observed mobility is very low for both n - and p -type samples.^{4,5} This is naturally explained by the bandwidths of the uppermost valence band and the minority-spin d bands being very narrow as shown in Fig. 3.

One of the prominent features of the calculated band structure is that the gap is very small (0.3 eV). It seems highly probable for CuFeS_2 to become a degenerate semiconductor as suggested by Teranishi and Sato.⁴ However, the degree of accuracy in the present calculation prevents definitive conclusions

for this problem. Another prominent feature is that the minority-spin d orbitals of Fe mix strongly into the upper valence bands and the occupation number of the orbitals have strong \vec{k} dependence (Fig. 4) as expected from delocalized orbitals. The departure of the magnetic moment from the value of an Fe^{3+} ion also comes from the delocalization of the minority-spin d electrons of Fe.

ACKNOWLEDGMENTS

We would like to express our sincere thanks to Dr. Teruo Teranishi and Dr. Katsuaki Sato for their continuing interests and invaluable discussions. We would like to thank Dr. H. Adachi, Professor M. Tsukada, and Dr. C. Satoko for their valuable discussions. Our gratitude is also due to Professor A. Yanase of Tohoku University for his kind allowance for use of the computer programs to construct the symmetrized basis functions in the crystal. This research was supported in part by a grant from Broadcasting Science Research Laboratories of NHK (Japanese Broadcasting Corporation). Numerical calculations were carried out on M-200H of the Institute for Molecular Science.

*To whom correspondence should be addressed.

¹C. H. L. Goodman and R. W. Douglas, *Physica (Utrecht)* **20**, 1107 (1954).

²I. G. Austin, C. H. L. Goodman, and A. E. Pengelly, *J. Electrochem. Soc.* **103**, 609 (1959).

³T. Teranishi, K. Sato, and K. Kondo, *J. Phys. Soc. Jpn.* **36**, 1618 (1974).

⁴T. Teranishi and K. Sato, *J. Phys. (Paris)* **36**, C3-149 (1975).

⁵T. Teranishi, *J. Phys. Soc. Jpn.* **16**, 1881 (1961).

⁶G. Donnay, I. M. Corliss, J. D. H. Donnar, N. Elliot, and J. M. Hastings, *Phys. Rev.* **112**, 1917 (1958).

⁷M. DiGiuseppe, J. Steager, A. Wold, and E. Kostiner, *Inorg. Chem.* **13**, 1828 (1974).

⁸D. Raj, K. Chandra, and S. P. Puri, *J. Phys. Soc. Jpn.* **24**, 39 (1968).

⁹T. Kambara, *J. Phys. Soc. Jpn.* **36**, 1625 (1974).

¹⁰T. Kambara, K. Suzuki, and K. I. Gondaira, *J. Phys. Soc. Jpn.* **39**, 764 (1975).

¹¹D. E. Ellis and G. S. Painter, *Phys. Rev. B* **2**, 2887

(1970).

¹²A. Zunger and A. J. Freeman, *Phys. Rev. B* **15**, 5049 (1977).

¹³H. Adachi, M. Tsukada, and C. Satoko, *J. Phys. Soc. Jpn.* **45**, 875 (1978); **45**, 1333 (1978).

¹⁴T. Oguchi, T. Kambara, and K. I. Gondaira, *Phys. Rev. B* **22**, 872 (1980).

¹⁵A. R. Rosen, D. E. Ellis, H. Adachi, and F. W. Averill, *J. Chem. Phys.* **65**, 3629 (1976).

¹⁶Similar tables for the wave functions at the X and Z points, and along the Λ and Δ lines are available on request.

¹⁷K. Sato and T. Teranishi, *J. Phys. Soc. Jpn.* **40**, 297 (1976).

¹⁸T. Oguchi, K. Sato, and T. Teranishi, *J. Phys. Soc. Jpn.* **48**, 123 (1980).

¹⁹G. F. Koster, J. O. Dimmock, R. G. Wheeler, and H. Statz, *Properties of the Thirty-Two Point Groups* (MIT Press, Cambridge, Mass., 1963).